

ARTICLE

Study of Atmospheric Variables using Low-Cost Stratospheric Balloon-Borne Missions

Rupnath Sikdar *, Sourav Palit, Sandip Kumar Chakrabarti, Debashis Bhowmick

Indian Centre for Space Physics, 466, Barakhola, Netai Nagar, Kolkata 700099, West Bengal, India

ABSTRACT

A better understanding of atmospheric dynamics and improvement of regional weather and climate models require accurate measurement and analysis of atmospheric variables such as temperature, pressure, and wind velocity across altitudes. In this study, we present such results from a series of high-altitude balloon missions conducted by the Indian Centre for Space Physics (ICSP). These missions, in which balloons reach up to altitudes of 42 km, provide high-resolution vertical profiles of atmospheric parameters over the Indian subcontinent, a region where such data are sparse. We analyze the payload's vertical ascent rates, horizontal displacements, and variations in some atmospheric parameters, such as temperature, pressure, and wind velocity with altitude. Wind velocity components—zonal (east-west) and meridional (north-south)—are also examined, with particular emphasis on their seasonal variability due to subtropical jet streams during pre- and post-monsoon periods. Our analysis reveals significant seasonal variation in wind patterns at stratospheric heights. We obtain clear indications that the atypical wind behaviors observed in 2019 may be linked to anomalies in monsoonal rainfall patterns. These results contribute valuable insights into upper atmospheric dynamics over the Indian region and also highlight the importance of balloon-borne observations in refining regional atmospheric models.

Keywords: Pressure and Temperature sensors; Weather Parameters; Wind Velocity; Stratospheric Balloon Missions

*CORRESPONDING AUTHOR:

Rupnath Sikdar, Indian Centre for Space Physics, 466, Barakhola, Netai Nagar, Kolkata 700099, West Bengal, India;
Email: rupnathsikdar1994@gmail.com

ARTICLE INFO

Received: 10 May 2025 | Revised: 27 June 2025 | Accepted: 7 July 2025 | Published Online: 18 July 2025
DOI: <https://doi.org/10.30564/jasr.v8i3.9633>

CITATION

Sikdar, R., Palit, S., Chakrabarti, S.K., et al., 2025. Study of Atmospheric Variables using Low-Cost Stratospheric Balloon-Borne Missions. Journal of Atmospheric Science Research. 8(3): 36–48. DOI: <https://doi.org/10.30564/jasr.v8i3.9633>

COPYRIGHT

Copyright © 2025 by the author(s). Published by Bilingual Publishing Group. This is an open access article under the Creative Commons Attribution-NonCommercial 4.0 International (CC BY-NC 4.0) License (<https://creativecommons.org/licenses/by-nc/4.0/>).

1. Introduction

For a range of scientific applications, including climate modelling, weather prediction, and studies of atmospheric dynamics, understanding the vertical structure of the Earth's atmosphere is necessary. This includes variations in temperature, pressure, and wind velocity with altitude. However, over the Indian subcontinent, ground-based high-resolution measurements extending into the stratosphere remain relatively sparse. So, more localized, cost-effective atmospheric profiling is needed to validate global models and enhance regional forecasting capabilities.

With the aim of addressing these gaps, the Indian Centre for Space Physics (ICSP) has been working on operating a series of low-cost, lightweight, high-altitude balloon experiments and is also in the process of establishing a dedicated stratospheric balloon facility in the state of West Bengal in India. The series of balloon missions operated so far has been collectively known as “Dignity” missions. There have been 114 such successful balloon flights. These balloons with payloads typically reach altitudes of up to 42 km and probe the middle and upper atmosphere. Significant contributions to our understanding of the space and atmospheric processes^[1–9] have already been made by some earlier balloon missions.

The primary scientific goals of the present study are

- (1) Analyze the vertical profiles of atmospheric temperature and pressure up to 35–40 km altitude and compare them with established atmospheric models such as the U.S. Standard Atmosphere (U.S. Government Printing Office, 1976^[10]), International Standard Atmosphere (ISO Technical Committee, 1975^[11]), and the NASA MSIS model.
- (2) To examine the wind speed and directional response, particularly in relation to the subtropical jet stream during pre- and post-monsoon periods over eastern India.
- (3) To evaluate whether balloon-borne data sets can potentially be used in refining regional atmospheric forecasts, especially those related to monsoonal dynamics.

Atmospheric parameters such as temperature, pressure, and wind velocity vary significantly with location and season due to differences in solar position, topography, and regional climate processes. Most notably, weather variability around monsoon in India is strongly influenced by upper tropospheric^[12–15] and lower stratospheric winds. These are

poorly constrained by satellite or radiosonde^[16] data alone. Direct measurement of these parameters at high vertical resolution from balloon platforms can thus contribute to improving long-term monsoon modeling and weather forecasting. This motivates our study objective stated above.

In this study, detailed observational results from selected balloon flights launched from ICSP's facility are presented. The measurements include temperature and pressure profiles obtained using onboard sensors and wind data obtained from in situ observations. These results are critically analyzed and compared with standard atmospheric models to assess their validity in the Indian context. The observed wind velocity profiles are corroborated with those from external sources such as the Wyoming Weather Web (https://weather.uwyo.edu/upperair/sounding_legacy.html, 2024^[17]).

The remainder of the paper is organized as follows: Section 2 provides an overview of the Dignity mission architecture, and Section 3 details the instrumentation. Section 4 discusses payload trajectories and atmospheric data analysis. In Section 5, we present a comparative discussion with global models and prior results. Section 6 outlines the limitations of our current study, and Section 7 concludes with key findings and implications for future work.

2. Missions Description

The motivation behind our small stratospheric balloon-borne experiments, instrumentation, and other mission details is discussed in Chakrabarti et al.^[4,5], and Bhowmick et al.^[18]. In this article, we briefly describe the relevant information on the missions and instruments we are dealing with. Our payloads are compact, lightweight (2–5 kg), and reusable as they are recovered from the landing location. Thus the recurring cost is very low (USD 700-900 per flight).

For the specified balloon missions discussed in this work, the operations involve ascending and descending from the ground to an altitude of ~42 km within an air corridor defined by the coordinates (22°N86°E, 22°N89°E, 24°N86°E, and 24°N89°E). This encompasses an area extending approximately 180 kilometres eastward, 52 kilometres to the north, 159 kilometres westward, and 160 kilometres to the south of the launch site, as depicted in **Figure 1**.

Balloon flights are conducted using three distinct con-

figurations. The first configuration involves a single rubber balloon paired with one parachute. The other two configurations utilize either one or two rubber balloons, which can carry payloads of approximately 2.5 kg and between 3 and 3.6 kg, respectively. If the payload weight is greater than 4 kg, then we use a TIFR-made polythene balloon of volume $\sim 4000 \text{ m}^3$. The prediction of the flight and landing location is conducted using two methods: one through a web-based platform (<https://predict.sondehub.org/>) and the other by analyzing in-situ wind velocity. Additionally, live locations

recorded from the receiving antenna and walkie-talkies provide real-time information on the flight path and landing site. Flight duration is around 3 – 5 hours for missions consisting of one rubber balloon and 5 – 7 hours for those consisting of two rubber balloons or a single plastic balloon. **Figure 2** shows the image of a balloon in flight photographed just after launch (left) and the scientific payload (right) kept inside a styrofoam box. **Table 1** represents some information about the missions that are used for data analysis purposes in this paper.

Table 1. Information about the specific Dignity missions.

Mission (No.)	Date [‡]	Launch Time (UT)	Landing Time (UT)	Launch Site [¶] (Lat, Lon)	Landing Location (Lat, Lon)
D56 (1)	10-12-2013	05:49:42	08:37:50	Kulti (23.73N, 86.84E)	23.63N, 88.26E
D75 (2)	14-05-2015	05:42:26	08:26:19	Muluk (23.65N, 87.71E)	23.68N, 88.08E
D76 (3)	15-05-2015	05:48:08	09:55:25	Muluk (23.65N, 87.71E)	23.85N, 88.05E
D77 (4)	15-05-2015	05:50:23	09:50:29	Muluk (23.65N, 87.71E)	23.78N, 88.06E
D78 (5)	16-05-2015	05:07:24	07:50:49	Muluk (23.65N, 87.71E)	23.03N, 88.78E
D82 (6)	19-05-2015	03:59:11	07:37:35	Muluk (23.65N, 87.71E)	23.63N, 88.26E
D83 (8)	20-11-2015	04:13:17	07:44:56	Muluk (23.65N, 87.71E)	23.75N, 88.07E
D84 (9)	20-11-2015	03:47:10	07:30:45	Muluk (23.65N, 87.71E)	23.69N, 88.07E
D86 (10)	20-11-2015	04:58:30	07:48:44	Muluk (23.65N, 87.71E)	23.80N, 88.05E
D87 (11)	20-11-2015	05:43:00	08:39:53	Muluk (23.65N, 87.71E)	23.85N, 88.07E
D88 (12)	21-11-2015	05:45:41	08:41:28	Muluk (23.65N, 87.71E)	23.84N, 88.08E
D90 (13)	09-05-2016	05:08:24	08:34:39	Muluk (23.65N, 87.71E)	23.81N, 88.09E
D91 (14)	10-05-2016	05:04:42	08:27:46 ^a	Muluk (23.65N, 87.71E)	23.86N, 88.11E

[‡] Date in day-month-year format; [¶] All locations are in West Bengal, India.; ^a A long flight with a duration of approximately eight hours

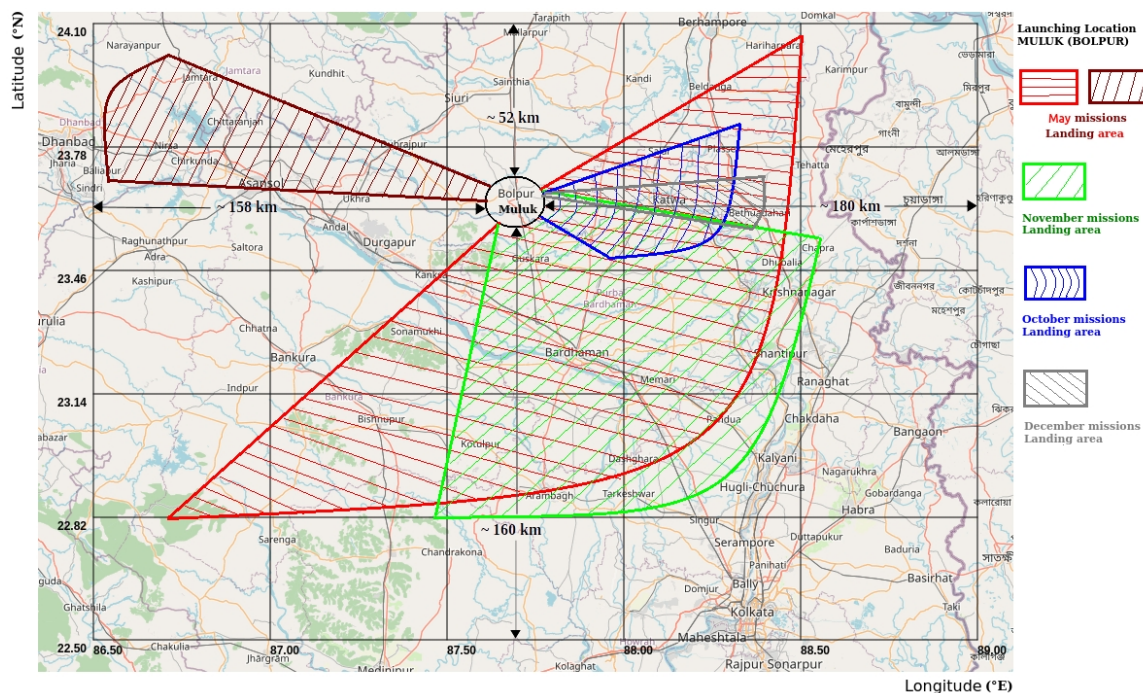


Figure 1. Air corridor designated for scientific ballooning from Bolpur, India.

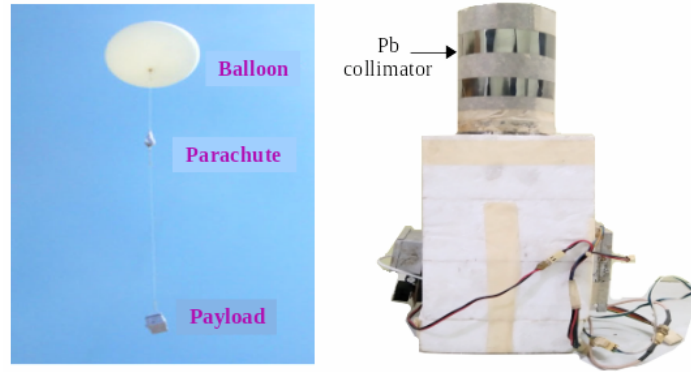


Figure 2. Left: a photo of a rubber balloon after launch. Right: A complete payload inside a thermocol box with a collimator.

3. Instruments

The main scientific instrument of the mentioned balloon missions is a scintillation detector, which detects X-rays and gamma-rays. The X-ray detectors are demonstrated in detail in Bhowmick et al.^[18]. In the present paper, however, we deal with the data procured from ancillary equipment such as pressure and temperature sensors and the GPS (Global Positioning System) unit. A temperature sensor is a device with a semiconductor-based integrated circuit containing two similar diodes. This sensor detects changes in current flow when exposed to temperature variations. To convert this current into a voltage suitable for measurement, a series resistor is used in conjunction with the transducer. The resulting voltage is then sent to an Analog-to-Digital Converter (ADC) for processing. After the conversion, the signal is saved in the storage media by the onboard computing unit. The pres-

sure sensor is a piezoresistor, made from semiconductor, and works on the piezoresistive effect, which provides a response in terms of voltage change subject to some mechanical forces acting on it. The force exerted by the air on the diaphragm of the pressure sensor causes a change in resistance. This change is an analogue signal that is sent to an analog-to-digital converter (ADC) to be transformed into a format that the onboard computer can understand. The digital data is then stored on solid-state storage media onboard. The GPS information (latitude, longitude, and altitude at every second) is read into the system from the GPS module, which is embedded in a microcontroller (a low-cost, small microcomputer). **Figure 3** indicates the complete block diagram of the whole design of the signal readout system. Other equipment, such as the 9DOF, GPS, clock module, HD cameras, etc., are also installed onboard.

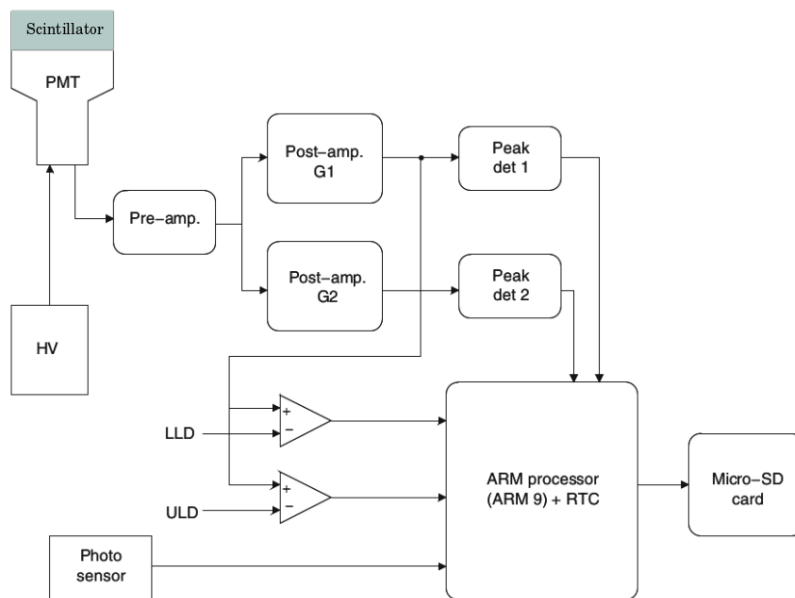


Figure 3. Complete block diagram of a typical balloon mission readout system.

4. Horizontal and Vertical Displacements of Scientific Payloads and Vertical Velocity

In a balloon mission, we procure the data of the horizontal and vertical displacements (altitude change) of the payload from the onboard GPS. **Figure 4** shows the horizontal displacement relative to latitude and longitude and corresponding vertical height with respect to time (IST) in ks (1000s) from launching to landing of the missions D56, D83, and D113. In this figure, in the upper panel for mission D56, the ascent rate is slow compared to the descent rate, so we obtained a lower horizontal displacement between launching and burst than between burst and landing. The opposite happens for mission D113, as seen in the lower

panel. In the middle panel for mission D83, the ascent rate and the descent rate are approximately the same; hence, the horizontal displacement between launch to balloon burst and burst to land is nearly the same. These things are controlled by the weather parameters, such as the wind speed, wind direction, balloon size, and number of balloons used in each mission. The vertical velocity, or ascent rate, has remained relatively stable throughout the mission's ascent phase for all the missions. As illustrated in the right panel of **Figure 4**, the typical ascent rate at lift-off is approximately 4 to 4.5 m/s, which then increases with altitude, reaching around 6 to 7 m/s at an altitude of ~ 30 km. During the mission, we need to determine the ascent and descent rates in situ to predict the flight path and ensure payload recovery for the balloon experiments.

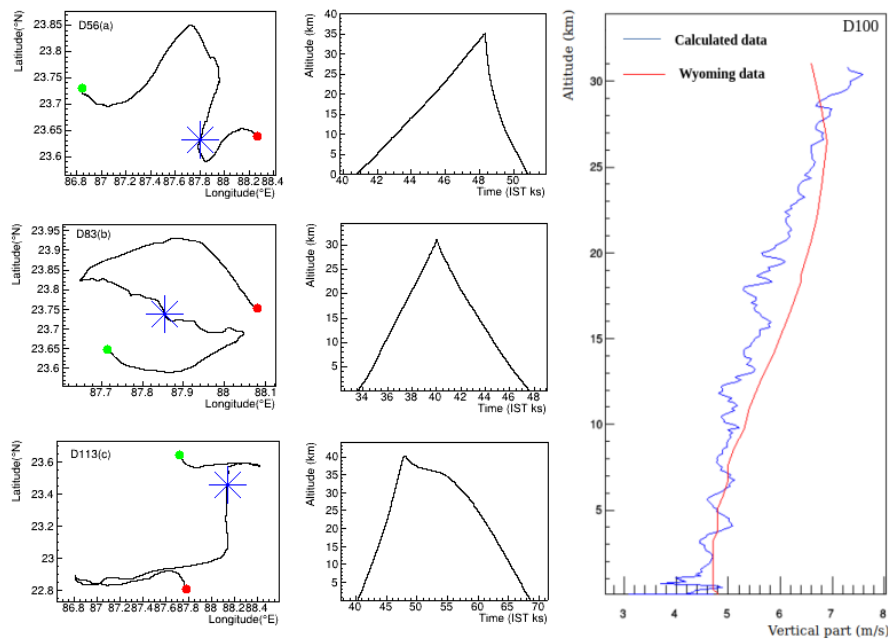


Figure 4. Left: Horizontal and vertical displacements for missions D56, D83, and D113. The red ball, blue star, and green ball are the locations of launching, burst, and landing for the specified missions respectively. Maximum altitude is ~ 42 km (for D113). Right: The vertical velocity profile is derived from GPS data for the D100 mission, compared with the Wyoming data plot. The figures vary due to wind patterns, behavior, and ascent and descent rates.

5. Atmospheric Data Analysis

To understand atmospheric and climate dynamics, we need to measure various atmospheric components, such as pressure, temperature, humidity, wind direction, and wind velocity. This data is collected from weather balloon missions conducted by ICSP, extending from the ground to approximately 30 km in altitude. Studying the variations in pressure and temperature

is crucial. For instance, high pressure typically signifies clear skies, while low pressure is often associated with storms. Water vapor, typically formed near the surface in conditions of high temperature and humidity, rises to higher layers of air. This movement causes convective instability, resulting in a decrease in surface pressure. While temperature generally decreases with altitude, it can occasionally rise due to pollutants. In the stratospheric region, temperatures increase again due to ozone

absorbing ultraviolet (UV) radiation. Tracking weather systems like cyclones, anticyclones, fronts, and storm systems is essential for forecasting precipitation, predicting rain, and understanding heat dynamics. Additionally, studying wind patterns is vital for investigating tornadoes (through wind shear), thunderstorms, jet streams (which influence storm paths and intensity), and for understanding air circulation, pollution dispersion, and broader climate studies. Considering these factors, we are excited to analyze the atmospheric data collected from our meteorological mission at ICSP. First, we have analyzed the pressure and temperature sensor data and the GPS data, helping us determine the wind velocities in the atmosphere. Observations of atmospheric parameters such as pressure and temperature with respect to altitude are discussed in Subsection 5.1. Two zonal and meridional components of the wind velocity as a function of altitude are measured during the pre- and post-monsoon seasons and are presented in Subsection 5.2.

5.1. Atmospheric Temperature and Pressure

We have discussed earlier the temperature and pressure sensors in our payload box and how they work (also see Chakrabarti et al.^[5]). We use the data from these sensors

directly for the measurement of pressure and temperature. Temperature and pressure are known to vary with payload altitudes as well as the latitudes^[19] of the geographic coordinate system. Here we present our analysis on data from a mission (D93) on how temperature and pressure change with vertical height from the Earth's surface and compare them with those derived from other models. In **Figure 5**, we overlay the temperature profile from the D93 missions with the temperature profile generated by the NRLMSIS 2.0 model^[20]. We selected this model because it is the most well-known and accurate empirical atmospheric model, providing a description of the average spatiotemporal behavior of the atmosphere. The pressure profile for this mission, along with the pressure profile from the U.S. standard model (Engineeringtoolbox.com, 2023^[21]), is illustrated in **Figure 6**. In this figure, there is a slight deviation in pressure from the U.S. standard model that occurs at altitudes between 15 and 20 km. This change is observed in the region known as the Regener-Pfotzer maximum^[22,23], where the secondary cosmic ray flux reaches its peak^[24]. This phenomenon may be attributed to the effect of high-intensity radiation surrounding the piezoelectric pressure sensor^[5,25].

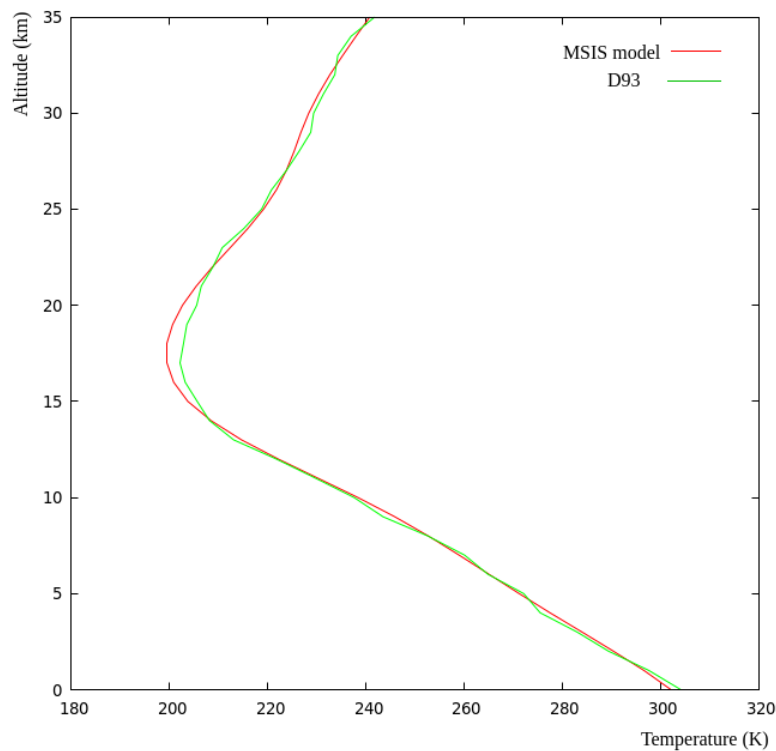


Figure 5. The NASA MSIS atmospheric profile (red) is superimposed on the temperature plot of mission D93 (green).

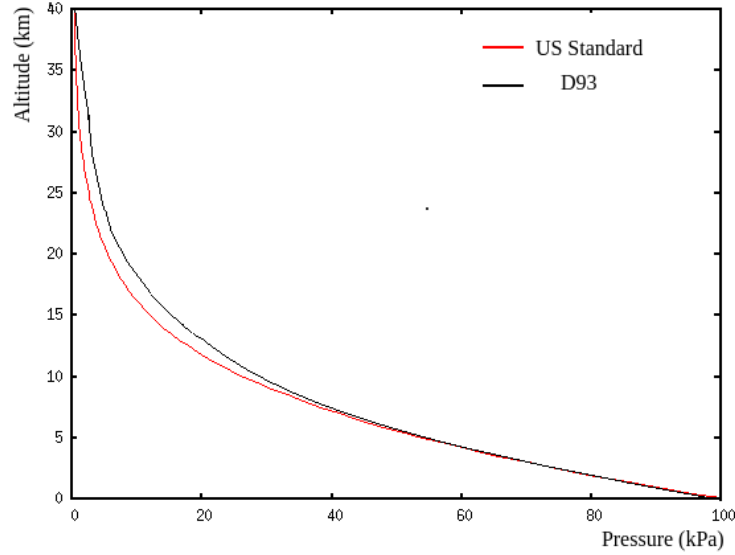


Figure 6. A pressure profile of mission D93 (black) with U.S. standard modelling (red) pressure data. The experimental data and model data show maximum deviation at the Regener-Pfotzer maximum, around 20 ± 5 km, due to the heightened ionization energy.

5.2. Wind Velocity

For the study of wind profiles, we collected wind data during the pre-monsoon and post-monsoon periods of the years 2015, 2016, and 2019. According to the Indian Meteorological Department (IMD), the monsoon rainfall was approximately normal for these years. We calculated two components of wind velocity: the zonal component (V_x in m/s) and the meridional component (V_y in m/s) using the relationships provided by the GPS data, which are defined as follows:

$$V_x = (d_{lon}/d_{tim}) \times 111139, \quad (1)$$

$$V_y = (d_{lat}/d_{tim}) \times 111139, \quad (2)$$

where, d_{lon}/d_{tim} and d_{lat}/d_{tim} are the changes in longitude in degrees and latitude in degrees with respect to time. We use the general velocity relationship, which is the rate of change of a variable (e.g., V_x), and the number 111139 comes from the equation $2\pi r/360 \approx 111139$, where $r = 6371$ km, the radius of Earth, in equations 1 and 2 for the transformation from degree to meter. For the calculation and averaging of the wind velocity, the averaging time span was chosen to be 30 seconds. The data obtained on wind velocity components are highly accurate, particularly for the zonal component, as demonstrated by the comparison in **Figure 7**, in which

we utilize two different data sources: one from our GPS, calculated with the above equations, and the other obtained directly from the Wyoming site for mission D100.

We could not observe the monsoonal low-level jet^[14] because our data are only taken during the pre- and post-monsoon seasons. We took the ascent data of the missions up to 30 km. For various missions, the maximum altitude (balloon burst height) obtained is above 30 km, and some reach up to ~ 42 km. We take the data up to 30 km for our analysis of all specified missions to get a better comparison. Missions D75, D76, D77, D78, D80, D81, D82, D83, and D84 conducted in May 2015 are considered pre-monsoon ones, while missions D86, D87, and D88 conducted in November 2015 are taken for post-monsoon. In 2016, we considered the missions in May (D90, D91, D92, D93, D94, and D95) for pre-monsoon and in October November (D96, D97, D98, D99, D100, and D101) for post-monsoon. Three missions (D110, D111, and D112) in May 2019 were taken for the pre-monsoon period. Only one mission (D113) in November 2019 is considered post-monsoon. For each of the years, we calculate the average wind velocity components for both the groups (pre- and post-monsoon mission data). We use here the usual sign convention of zonal and meridional, which is also used in Ruchith et al.^[14] Zonal wind is positive (westerly) and negative (easterly) if it blows from west to east and east to west, respectively. On the other hand, negative (northerly) meridional values indicate wind blowing from

north to south, and positive (southerly) meridional values indicate wind blowing from south to north. In the vertical profile (**Figure 7**) of zonal and meridional components, we say that the wind is southwesterly. The southwesterly wind associated with the Asian monsoon is primarily a result of thermal differences between the continent and the ocean in both summer and winter surface conditions, as described in the article by Tarakanov^[26]. During the summer, when the ocean has not yet warmed up and the air pressure above it remains high, air moves from the cooler Indian Ocean towards the warmer landmass of the Hindustan Peninsula. This is why the summer Asian monsoon typically features a southwesterly direction for surface winds. The intense heating of the land surface, driven by solar radiation, leads to a significant decrease in atmospheric pressure at the surface. This, in turn, creates a high-pressure area at altitudes of 3-5 kilometres. The lower boundary of the subtropical jet stream exists at altitudes of 5-7 kilometres, and the change in airflow at the lower altitude shifts to a northeasterly direction. In the summer, the influence of the subtropical jet stream can be diminished by increased air turbulence. This turbulence often leads to the formation of surface thunderstorms, which can produce intense precipitation. Indeed, the precipitation can significantly lower the surface air temperature, which can contribute to a slight increase in surface atmospheric pressure. However, water vapor, usually formed near the surface against a background of high temperature and humidity, rushes to higher layers of air, causing convective instability and, as a result, further lowering surface pressure.

During the pre-monsoon and post-monsoon periods, the zonal component of the wind (as shown in the left panel of **Figure 8** and **Figure 9**) at the upper troposphere, specifically within the tropopause height range of 10 to 15 km, is predominantly westerly. This westerly wind is influenced by the subtropical westerly jet streams that occur in summer over India, with maximum intensity found at an altitude of approximately 12 km. This observation is consistent with the findings reported by Ruchith et al.^[14]. Above an altitude of around 20 km, the wind velocity (zonal) is nearly steady and easterly.

The Figures show that the magnitude of the meridional component of wind is generally smaller compared to that of the zonal component, particularly in the lower troposphere. During the pre-monsoon in 2015, the surface

wind was northerly up to 10 km. Then southerlies prevailed for 10 – 20 km; thereafter, the wind turned northerly and again southerly. Winds are mainly from the south at up to 20 km, though they are weaker than zonal winds. During the post-monsoon period in 2015, northerly winds prevailed almost throughout the troposphere and had magnitudes lower than the pre-monsoon. The wind behavior during the pre-monsoon and post-monsoon seasons in 2016 was nearly the same as in 2015. In the pre-monsoon of 2019, for the meridional component (green line in the right panel of **Figure 8**), winds are southerly with a significant magnitude of around 17 m/s at ~ 13 km because of the late arrival (8th June) of the south-west monsoon in Kerala, India. In addition, there was overall significant variation in the meridional wind for mission D113, executed in post-monsoon in 2019, from the meridional wind of the previous years.

It is noted that the 2019 wind velocity components (particularly the meridional components) in the pre- and post-monsoon seasons deviate from those of the other two years very significantly. The Indian Meteorological Department (IMD) data (Reliefweb.int/report/india/2019-southwest-monsoon-season-rainfall-and-imd-s-long-range-forecasts,2024^[27]) indicates that in 2019, the onset of the monsoon was late and a large deficiency in rainfall was recorded in the month of June. Even though, in July, August, and September, the rainfall was much above the normal, and the overall rainfall was 110 percent of its Long Period Average (LPA) (the highest after 1994). Indeed, in the month of September 2019, the rainfall was 152 percent of the LPA for the month (the highest after 1917). We conjecture that the deviations we find in both pre- and post-monsoon wind patterns in 2019 may be related to the anomalous rainfall pattern reported by IMD^[27]. Rain and humidity can affect wind direction by changing the pressure distribution in the atmosphere. Relatively lower humidity (compared to previous years) in the pre-monsoon session of 2019 may have caused a larger tropospheric pressure gradient around the region, leading to higher meridional wind velocity. When rain falls, it can cause a low temperature in the air near the surface, leading to an increase in air pressure. It causes the wind to flow from high-pressure areas to low-pressure regions, affecting its direction, which can change the wind direction^[28]. Overall, the impact of rain and the rate of rainfall on wind velocity is complex and may vary depending on the specific

weather conditions and the location of the rain. A definite conclusion on the observed variation and correlation requires examining many more years of wind and rainfall data. Through our upcoming balloon missions, we aim to build a comprehensive wind velocity database to analyze and better

understand these variations and correlations. Variability in rainfall across the European part of Russia has been shown to correlate with the thermal conditions of North Atlantic waters and atmospheric circulation patterns from 1896 to 2003, as noted by Kondratovich & Kulikova^[29].

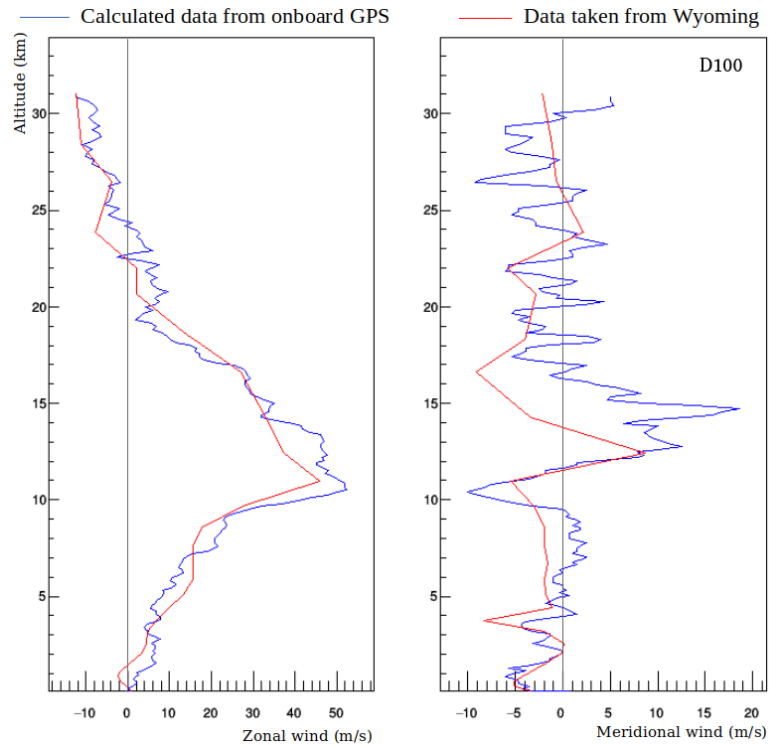


Figure 7. The comparison of computed wind speeds along the x (zonal) and y (meridional) axes using both experimental data and Wyoming data.

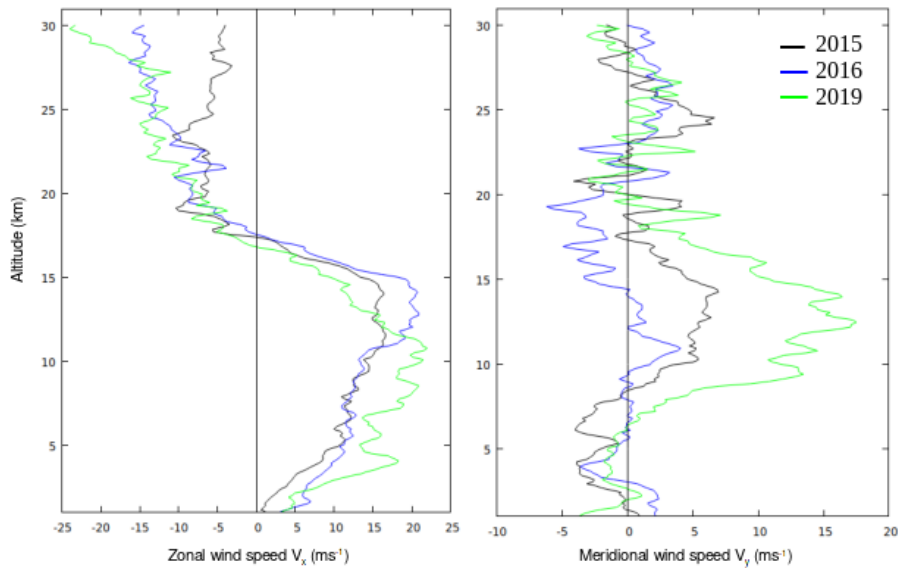


Figure 8. The mean profiles of the two wind velocity components (zonal and meridional) are shown in the left and right panels, respectively, using the data of 2015 (black lines), 2016 (blue lines), and 2019 (green lines) during the pre-monsoon season.

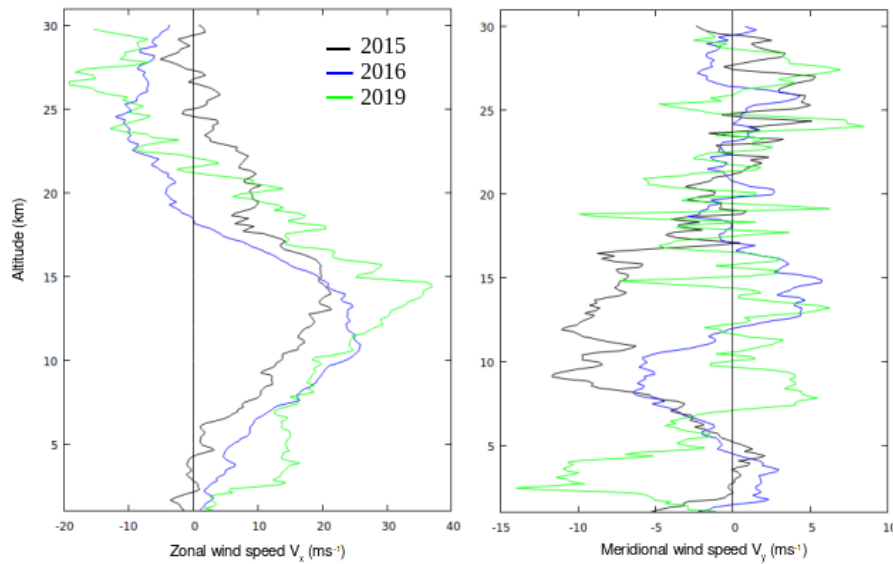


Figure 9. The mean profiles for two wind velocity components (zonal and meridional) are shown in the left and right panels, respectively, using the data of 2015 (black lines), 2016 (blue lines), and 2019 (green lines) during the post-monsoon season.

6. Limitations of the Study

There are many limitations present in our present study using balloon-borne missions, which we are planning to overcome in future missions. Firstly, we have no long-term continuous data during the pre- and post-monsoon, which could have given us a deeper understanding of the analyzed outcome. Secondly, we have not been able to find the impact of thunderstorms on wind velocity and direction, as we could not get a chance to conduct any missions on thunderstorm days. We do not calculate the wind velocity in conventional methods and compare it with other agencies like IMD; we only calculate the two components of wind velocity from the movement of balloons measured by GPS and present the details of their variation with altitude at different seasons (pre- and post-monsoon). Albeit our wind velocity observations agree with the results presented in existing literature such as Ruchith et al. [14].

7. Conclusions

In this article, we present the measurement of some atmospheric variables (temperature, pressure^[5], wind velocities^[2,4,5,30]) and some physical quantities related to balloon motion (e.g., horizontal displacement) that depend on the atmospheric conditions. Pressure and temperature with respect to altitude are usually measured by radiosondes. However, our sensors are accurate enough to observe and compare

these variables during pre- and post-monsoon seasons. We show the presence of westerly and easterly subtropical jet streams during summer (altitude at around 12 – 15 km) using some missions that were carried out in May. Meridional components were determined using the October and November mission data, which fluctuated northerly and southerly with a small magnitude compared to zonal during the pre- and post-monsoon seasons. The role of the subtropical jet stream in the formation of the intense summer monsoon is certainly significant, especially in recent years. It would be valuable to track this contribution from 2000 to 2025 by increasing the number of stratospheric pilot balloon launches and their frequency within a single day. Additionally, it would be beneficial to place launch points not only in West Bengal but also in the western states of India. These results hold considerable significance as they deepen our scientific understanding of atmospheric characteristics. Our study draws from an extensive data set that spans from 2013, encompassing the findings from not just a solitary balloon mission but an impressive total of fourteen distinct missions. This comprehensive approach allows us to gather a wealth of information that contributes to the overall analysis. Additionally, some important findings—like the analysis of wind speed from a single balloon mission—were already discussed in Chakrabarti et al. [3], which was based on data from just one flight. In our work, we used data from many missions, which helped us gain deeper and more detailed insights.

Thunderstorms may affect the wind velocity and direction. Thunderstorm activity typically occurs under conditions of minimal surface wind. Increased airflow during a thunderstorm is generally linked to a squall, which is characterized by a rapid increase in air movement caused by the movement of clouds. A squall can be thought of as a vortex that develops in a horizontal plane. However, determining the speed of airflow during a squall can be challenging because a squall is primarily a vortex rather than a straightforward flow of air. The wind results would be more accurate if we had the all-day database during the pre-monsoon (March-May) and post-monsoon (October-November). However, our 3- to 8-day averages of wind speed data show convincing results and follow the wind's behavior in the atmosphere. In the future, we will plan the mission's execution in the monsoon season on most days to study the monsoon low-level jet and the correlation between rainfall and winds. The article by Koteswaram & Parthasarathy^[31] analyzes the average jet stream over India during the pre-monsoon and post-monsoon seasons. It reveals that the westerly jet still exists but with reduced intensity. By utilizing Pibal data, the authors assess vertical motions and circulation patterns near the subtropical jet and anticyclone. The findings support the confluence mechanism for jet formation and link clear-air turbulence over India to the vertical motion patterns located south of the jet. The monsoon circulation is mainly influenced by local surface conditions, including radiative heat and the distribution of permanent atmospheric pressure centers. We will also aim to take the data for all days for pre- and post-monsoonal seasons and analyze and present the more refined and accurate results elsewhere in the future.

While comparing components of wind velocity in the pre- and post-monsoon seasons, we find significant deviations in the year 2019. The IMD data also indicated highly anomalous rainfall in that year. Where the data for the month of June shows a significant deficiency in rainfall, the September data shows 152 percent rainfall as compared to the LPA (the highest after 1917). We attempt to correlate the variation of our wind velocity data with the anomalous rainfall profile of that year. Future continuous observations will aid in understanding and establishing such a correlation much better. Such data can potentially be used in refining regional atmospheric forecasts, especially those related to monsoonal dynamics.

Author Contributions

The project was initially conceptualized and executed by S.K.C., with assistance from engineer D.B., before R.S. joined the team. After becoming part of the project, R.S. conducted data analysis and provided theoretical interpretations of the findings after downloading and processing the raw data into an accessible format. He also prepared the initial draft of the manuscript, which included figures and detailed descriptions. Subsequently, S.K.C. and S.P. revised and refined the manuscript into its final form. All authors reviewed the final results and approved the completed article.

Funding

Dr. Rupnath Sikdar sincerely appreciates the support from the University Grants Commission scholarship, which made this research possible.

Institutional Review Board Statement

Not applicable.

Data Availability Statement

All data and results presented in this study were obtained from the Indian Centre for Space Physics.

Acknowledgments

The authors would like to express their sincere gratitude to the team members of the ICSP Dignity Balloon Missions: Mr. A. Bhattacharya, Mr. S. Midya, Mr. H. Roy, Mr. R.C. Das, and Mr. U. Sardar. Their valuable assistance throughout the mission operations, execution, and data collection processes has been greatly appreciated.

Conflicts of Interest

We, the authors of this study, declare that we have no conflicts of interest, whether financial, professional, or personal, with any member of the editorial board or with any other contributing authors. We affirm that the integrity and objectivity of our research and its presentation have been maintained without any external influence. The authors con-

firm that there are no known financial conflicts of interest related to this work. This study was conducted independently and does not overlap with any other projects. All relevant references used in the preparation of this paper have been properly cited, and no external intellectual property has been utilized without appropriate acknowledgment.

References

- [1] Chakrabarti, S., Bhowmick, D., Sarkar, R., et al., 2011. High energy astrophysics with rubber balloons. In: Ouwehand, L. (ed.). *Proceedings of 20th Symposium on European Rocket and Balloon Programmes and Related Research*; May 22- May 26, 2011; Hyeres, France. ESA SP-700, 581-58.
- [2] Chakrabarti, S., Bhowmick, D., Palit, S., et al., 2013. A new paradigm in space based experiments using rubber balloons. In: Ouwehand, L. (ed.). *Proceedings of 21st ESA Symposium on European Rocket and Balloon Programmes and Related Research*; June 9- June 13, 2013; Thun, Switzerland, 663-670.
- [3] Chakrabarti, S., Bhowmick, D., Chakraborty, S., et al., 2014. Study of properties of cosmic rays and solar x-ray flares by balloon borne experiments. *Indian Journal of Physics*. 88, 333–341. DOI: <https://doi.org/10.1007/s12648-013-0424-z>
- [4] Chakrabarti, S., Bhowmick, D., Sarkar, R., et al., 2015. Unique high energy experiment initiative by ICSP with weather balloons. In: Ouwehand, L. (ed.). *Proceedings of the 22nd ESA Symposium on European Rocket and Balloon Programmes and Related Research*; June 7-12, 2015; Tromsø, Norway. ESA SP-730, 557.
- [5] Chakrabarti, S., Sarkar, R., Bhowmick, D., et al., 2017. Study of high energy phenomena from near space using low-cost meteorological balloons. *Experimental Astronomy*. 43(3), 311–338. DOI: <https://doi.org/10.1007/s10686-017-9540-7>
- [6] Sarkar, R., Chakrabarti, S.K., Pal, P.S., et al., 2017. Measurement of secondary cosmic ray intensity at Regener-Pfotzer height using low-cost weather balloons and its correlation with solar activity. *Advances in Space Research*. 60(5), 991–998. DOI: <https://doi.org/10.1016/j.asr.2017.05.014>
- [7] Sarkar, R., Chakrabarti, S., Bhowmick, D., et al., 2019. Detection of Crab radiation with a meteorological balloon borne phoswich detector. *Experimental Astronomy*. 47, 345–358. DOI: <https://doi.org/10.1007/s10686-019-09632-0>
- [8] Sarkar, R., Roy, A., Chakrabarti, S.K., 2020. Simulation of cosmic rays in the Earth's atmosphere and interpretation of observed counts in an X-ray detector at balloon altitude near tropical region. *Advances in Space Research*. 65(1), 189–197. DOI: <https://doi.org/10.1016/j.asr.2019.09.046>
- [9] Sikdar, R., Chakrabarti, S., Bhowmick, D., 2023a. Study of secondary cosmic rays using small stratospheric balloon missions. *Journal of Astrophysics and Astronomy*. 44. DOI: <https://doi.org/10.1007/s12036-023-09964-6>
- [10] U.S. Government Printing Office, 1976. *The U.S Standard Atmosphere*, Technical Memorandum (TM), ID – 19770009539, October 1, 1976.
- [11] ISO 2533:1975. 1975. *Standard atmosphere*.
- [12] Joshi, R., Singh, N., Deshpande, S., et al., 2006. UHF wind profiler observations of monsoon low level jet over Pune. *Indian Journal of Radio and Space Physics*. 35(5), 349–359. Available from: https://www.researchgate.net/publication/266618977_UHF_wind_profiler_observations_of_monsoon_low_level_jet_over_Pune (cited 1 October 2006).
- [13] Raj, P., Deshpande, S. M., 2008. Pre-monsoon to monsoon change in direction of vertical motions in the tropical lower troposphere from UHF radar observations. *Geophysical Research Letters*. 35. L15808, DOI: <https://doi.org/10.1029/2008GL034421>
- [14] Ruchith, R., Deshpande, S., Ernest Raj, P., 2016. UHF wind profiler observations of monsoon low-level jet (MLLJ) and its association with rainfall over a tropical Indian station. *Atmósfera*. 29(1), 1–9. DOI: <https://doi.org/10.20937/ATM.2016.29.01.01>
- [15] Manchanda, R.K., Subba Rao, J.V., Sreenivasan, S., et al., 2011. Study of seasonal variation of winds in upper stratosphere over Hyderabad. *Advances in Space Research*. 47(3), 480–487. DOI: <https://ui.adsabs.harvard.edu/abs/2011AdSpR..47..480M>
- [16] Survo, P., Hiltunen, E., Jauhainen, H., et al., 2014. Atmospheric temperature and humidity measurements of Vaisala Radiosonde RS41. *Proceedings of 17th Symposium on Meteorological Observation and Instrumentation*. Available from: https://www.researchgate.net/publication/284167391_ATMOSPHERIC_TEMPERATURE_AND_HUMIDITY_MEASUREMENTS_OF_VAISALA_RADIOSONDE_RS41 (cited 11 June 2014).
- [17] University of Wyoming, 2024. *Upper Air Soundings*. Available from: <https://weather.uwyo.edu/upperair/sounding.html> (cited 21 December 2024).
- [18] Bhowmick, D., Chakrabarti, S.K., Sarkar, R., et al., 2019. Development of instruments for space exploration using meteorological balloons. *Journal of Astronomical Telescopes, Instruments, and Systems*. 5(3), 1–16. DOI: <https://doi.org/10.1117/1.JATIS.5.3.036001>
- [19] Montgomery, K., 2006. Variation in temperature with altitude and latitude. *Journal of Geography*. 105, 133–135. DOI: <https://doi.org/10.1080/00221340608978675>
- [20] Emmert, J., Drob, D., Picone, J., et al., 2021. *NRLM-SIS 2.0: A whole-atmosphere empirical model of*

- temperature and neutral species densities. *Earth and Space Science*. 8. DOI: <https://doi.org/10.1029/2020EA001321>
- [21] Engineeringtoolbox.com, 2023. Standard atmosphere. Temperature, Pressure, and Air Properties vs. Altitude. Available from: https://www.engineeringtoolbox.com/standard-atmosphere-d_604.html (cited 13 May 2024).
- [22] Regener, E., 1933. New results in cosmic ray measurements. *Nature*. 132, 696–698. DOI: <https://doi.org/10.1038/132696a0>
- [23] Pfozter, G., 1936. Triple coincidences of ultraviolet radiation from a vertical direction in the stratosphere. *Zeitschrift für Physik*. 102, 41–58. DOI: <https://doi.org/10.1007/BF01336830>. (in German)
- [24] Carlson, P., Watson, A.A., 2014. Erich Regener and the ionisation maximum of the atmosphere. *History of Geo- and Space Sciences*. 5(2), 175–182. DOI: <https://doi.org/10.5194/hgss-5-175-2014>
- [25] Boychenko, D., Nikiforov, A., Skorobogatov, P., et al., 2007. Radiation effects in piezoelectric sensor. *Proceedings of the European Conference on Radiation and its Effects on Components and Systems (RADECS)*; September 10 – September 14, 2007; Deauville, France. pp. 1–4. DOI: <https://doi.org/10.1109/RADECS.2007.5205522>
- [26] Tarakanov, G.G., 1982. *Tropical Meteorology*, Mir Publishers: Moscow, Russia.
- [27] ReliefWeb, 2024. 2019 Southwest Monsoon Season Rainfall and IMD's Long-range Forecasts. Available from: <https://reliefweb.int/report/india/2019-southwest-monsoon-season-rainfall-and-imd-s-long-range-forecasts> (cited 21 December 2024).
- [28] Bartlett, H. J., 1914. The relation between wind direction and rainfall. *Q.J.R. Meteorol. Soc.*, 40: 327–346. DOI: <https://doi.org/10.1002/qj.49704017205>
- [29] Kondratovich K.V. and Kulikova L.A. 2008, On climatically significant changes in the moisture regime on the European territory of Russia in the 20th century. *Izvestiya RAN. Seriya geograficheskaya*, 2008, No. 1, pp. 73–76. (in Slovenian)
- [30] Sikdar, R., Chakrabarti, S., Bhowmick, D., 2023b. Study of solar flares and gamma-ray bursts using low-cost stratospheric balloon borne experiments. *Experimental Astronomy*. 56, 1–16. DOI: <https://doi.org/10.1007/s10686-023-09899-4>
- [31] Koteswaram, P., Parthasarathy, S., 1954. The mean Jet Stream over India in the pre-monsoon and post-monsoon seasons and vertical motions associated with sub-tropical Jet Streams. *Indian Journal of Meteorology and Geophysics*. MAUSAM, vol. 5, no. 2, pp. 138–156, Apr. 1954. DOI: <https://doi.org/10.54302/mausam.v5i2.4855>